

Giant Magnetotransport Phenomena in Filling-Controlled Kondo Lattice System: $\text{La}_{1-x}\text{Sr}_x\text{MnO}_3$

Yoshinori TOKURA^{1,2}, Akira URUSHIBARA¹, Yutaka MORITOMO²,
Takahisa ARIMA¹, Atsushi ASAMITSU², Giyu KIDO³ and Nobuo FURUKAWA⁴

¹*Department of Physics, University of Tokyo, Tokyo 113*

²*Joint Research Center for Atom Technology (JRCAT), Tsukuba 305*

³*National Research Institute for Metals, Tsukuba 305*

⁴*Institute for Solid State Physics, University of Tokyo, Tokyo 106*

(Received September 1, 1994)

Giant magnetotransport phenomena including the field-induced nonmetal-metal transition have been found in single crystals of $\text{La}_{1-x}\text{Sr}_x\text{MnO}_3$ near the critical composition ($x \approx 0.17$) for the nonmetal-metal transition and in the temperature region around the magnetic phase transition. Change of the resistivity shows a universal curve as a function of the magnitude of temperature- or field-induced magnetization, the most of which agrees with the prediction by the $D = \infty$ and $S = \infty$ Kondo lattice model with strong ferromagnetic (Hund) coupling.

[magnetoresistance, $\text{La}_{1-x}\text{Sr}_x\text{MnO}_3$, carrier doping, metal-insulator transition,
Kondo lattice, double exchange interaction]

Extensive studies on normal state properties of cuprate superconductors have aroused renewed interest in spin-charge-coupled dynamics near the Mott transition in 3d electron transition metal oxide systems with strong electron correlations. Among a number of metallic but strongly correlated 3d electron systems, hole-doped manganese oxides with perovskite structure, *e.g.* $\text{La}_{1-x}\text{Ca}_x\text{MnO}_3$ and $\text{La}_{1-x}\text{Sr}_x\text{MnO}_3$, are known to be conducting ferromagnets^{1,2)} in which the magnetic interaction is mediated by the so-called double exchange interaction between Mn^{3+} and Mn^{4+} ions.³⁻⁶⁾ In 1969 it was first reported⁷⁾ for one of these manganese oxides, $\text{La}_{1-x}\text{Pb}_x\text{MnO}_3$ ($x = 0.31$), that a large negative magnetoresistance (MR) is observed around the magnetic phase transition temperature. Much more recently, a similar or more pronounced MR has been confirmed for thin films of $\text{La}_{1-x}\text{Ca}_x\text{MnO}_3$ ^{8,9)} and $\text{La}_{1-x}\text{Ba}_x\text{MnO}_3$,¹⁰⁾ which may attract current interest in relation to possible application of the giant magnetoresistance (GMR) as well.

In this Letter, we report on the first quantitative explanation of the giant magnetotransport phenomena in the manganese oxide systems which were systematically investigated for filling-controlled single crystals of

$\text{La}_{1-x}\text{Sr}_x\text{MnO}_3$. In the single crystals immediately beyond the nonmetal-metal compositional phase boundary ($x = 0.17$), the low-temperature metallic resistivity decreases two orders of magnitude from the value above the magnetic transition temperature and the negative MR ($-\Delta\rho/\rho$) reaches >0.9 around T_c ($=200\text{--}350\text{ K}$). These anomalously large magnetotransport and temperature-dependent transport properties can be scaled to a universal curve as a function of the magnetization, which can be quantitatively evaluated by the Kondo lattice model with ferromagnetic coupling.

Let us begin with a quick review of fundamental electronic features in hole-doped manganese oxides such as $\text{La}_{1-x}\text{Sr}_x\text{MnO}_3$. The parent antiferromagnetic insulator LaMnO_3 involves Mn^{3+} ions with $t_{2g}^3 e_g^1$ ($S = 2$) configuration. Among the four $3d^4$ electrons on the Mn site, the Hund-coupled t_{2g}^3 electrons may be viewed as a single local spin ($S = 3/2$) because of their narrow one-electron bandwidth, while the e_g^1 state hybridized strongly with the O 2p states is either itinerant or localized. The end insulator LaMnO_3 is a Mott insulator due to strong correlations of the e_g electrons. However, the deviation of the e_g band filling

(n) from the integer value ($n=1$), that corresponds to the so-called "hole-doping" process in correlated insulators, may cause an insulator-to-metal transition. The distinct feature of such a barely metallic state in manganese oxides is that there is a strong exchange interaction (Hund coupling) between the itinerant e_g electrons (or holes) and t_{2g} spins. Hence, the following Kondo lattice Hamiltonian may well represent the electronic state for the hole-doped manganese oxide system,^{6,11)}

$$\mathcal{H} = - \sum_{\langle ij \rangle \sigma} t_{ij} (c_{i\sigma}^\dagger c_{j\sigma} + h.c.) - J \sum_i \sigma_i \cdot S_i. \quad (1)$$

Here, the first term represents the e_g electron transfer between neighboring sites i and j , while the latter shows the ferromagnetic ($J > 0$) Kondo coupling of the conduction e_g electron spin and localized t_{2g} ($S=3/2$) spin. The effect of the magnetic field (B) can be taken into account by adding the Zeeman term in eq. (1). An intuitive view on the MR effect obtained from this model is that the magnetic field tends to align the local spin and then the forcedly spin-polarized conduction electron suffers less from the scattering by local spins and becomes more itinerant.

Crystals of $\text{La}_{1-x}\text{Sr}_x\text{MnO}_3$ ($0 < x < 0.5$) were grown using the floating-zone furnace, details of which will be published elsewhere. To characterize the crystals, X-ray and neutron diffraction, electron probe microanalysis (EPMA) and titration analysis were carried out. The results indicated that the obtained crystals with $0 \leq x \leq 0.4$ show a composition nearly identical to the prescribed one. In particular, the x -value determined by the EPMA coincides with the prescribed one within an error of ± 0.01 . Furthermore, the magnetic transition temperature (T_c) as a function of x is in agreement with the results reported for ceramics samples.²⁾

In Fig. 1 we show temperature dependence of resistivity (ρ) in $\text{La}_{1-x}\text{Sr}_x\text{MnO}_3$ crystals with the compositions near the nonmetal-metal transition. A sharp drop in resistivity is observed immediately below the magnetic transition temperature T_c as indicated by arrows, which was determined by measurements of ac susceptibility. In particular, the low-temperature resistivity in the $x=0.175$ – 0.30 compounds is nearly two orders of magnitude

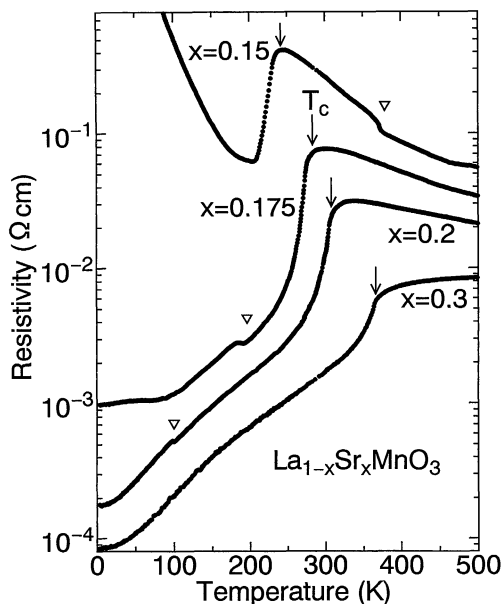


Fig. 1. Temperature dependence of resistivity in $\text{La}_{1-x}\text{Sr}_x\text{MnO}_3$ crystals near the nonmetal-metal compositional phase boundary. Triangles indicate small anomalies due to the structural phase transition from the rhombohedral to orthorhombic lattice.

smaller than that above T_c . Anomalies indicated by triangles in the figure are due to the structural transition of the slightly distorted perovskite from the rhombohedral (high-temperature phase) to orthorhombic (low-temperature phase) structure. The well-defined T_c as well as the well-defined structural phase transition temperature ensures that the composition of the sample is fairly homogeneous.¹²⁾

The marked drop in resistivity observed immediately below T_c is due to increase of the carrier mobility which results from decrease in the carrier scattering by thermal spin fluctuation. The double exchange theory⁴⁾ indicates that the effective electron (hole) transfer (\tilde{t}_{ij}) between the neighboring sites depends on the relative angle ($\Delta\theta_{ij}$) of the local (t_{2g}) spins as $\tilde{t}_{ij} = t_{ij} \cos(\Delta\theta_{ij}/2)$. Thus, the ferromagnetic spin arrangement tends to increase the effective spin transfer interaction and hence the hole mobility. This is the main cause of the rapid decrease of the resistivity immediately below T_c accompanied by the onset of the ferromagnetic spin moment (see also Fig. 3(a)). The samples with $x \leq 0.3$ show semiconducting behavior above T_c . This may be interpreted in

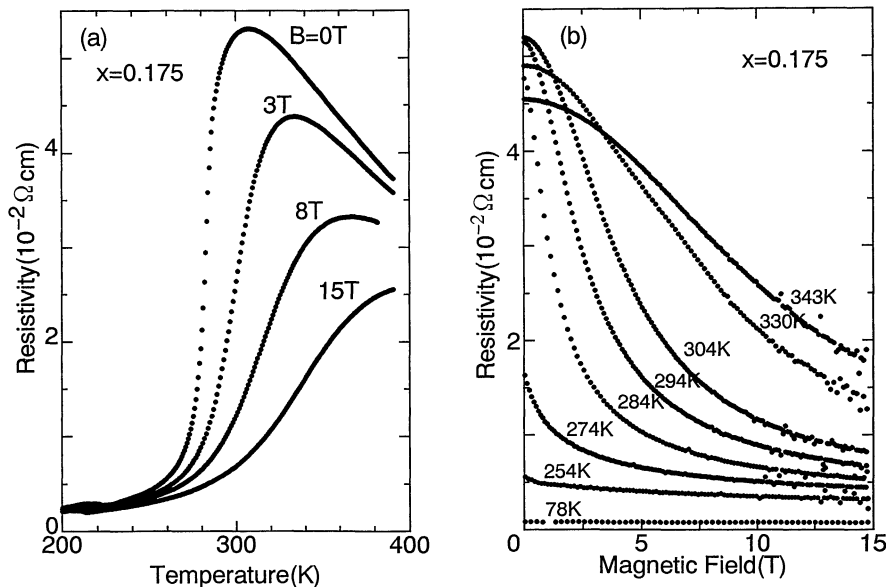


Fig. 2. Magnetoresistance in $\text{La}_{1-x}\text{Sr}_x\text{MnO}_3$ ($x=0.175$) crystal: (a) temperature dependence of resistivity in magnetic fields and (b) the magnetic field dependence of resistivity.

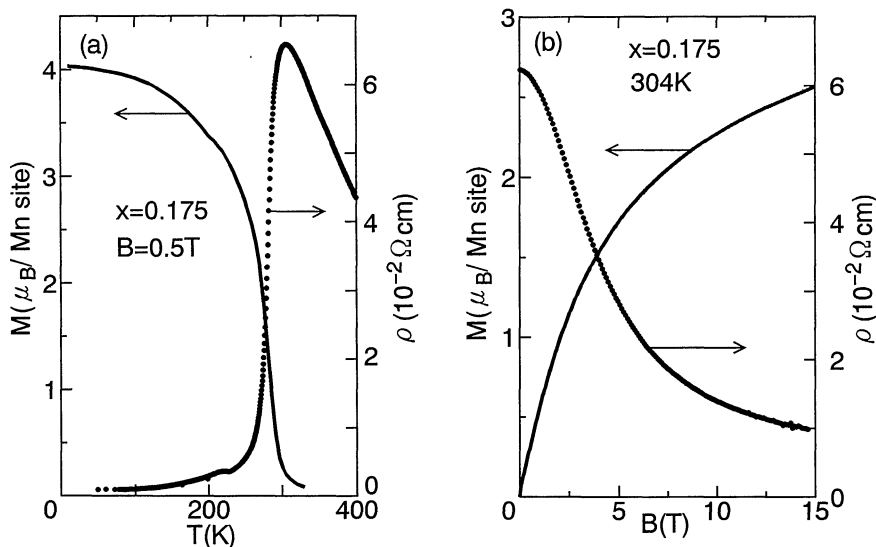


Fig. 3. Correlations between the changes of resistivity (ρ) and magnetization (M) per Mn site for $\text{La}_{1-x}\text{Sr}_x\text{MnO}_3$ ($x=0.175$) crystal: (a) temperature dependence of ρ and M in the bias field of 0.5 T and (b) field dependence of ρ and M at 340 K (above T_c).

terms of a localization effect of the e_g hole carriers with greatly reduced mobility due to the paramagnetic spin configuration.¹³⁾

We show in Fig. 2 an example of the magnetic field effect on the resistivity (the longitudinal MR; $I//B$) for the $x=0.175$ crystal which is

close to the nonmetal-metal compositional boundary. Anomalous large negative MR is observed around T_c . The MR was found to be nearly isotropic: The transverse MR is only a few percent smaller in absolute magnitude than the longitudinal MR. The MR magnitude

apparently corresponds to the change of magnetization which is large around T_c . In particular, the MR value defined as $[\rho(0) - \rho(B)]/\rho(0)$ is as large as 0.9 around T_c ($=283$ K). Such a giant MR phenomenon immediately above T_c may be viewed as the field-induced nonmetal-metal transition. By contrast, the MR effect at 78 K for the fully spin-ordered state is very small compared with that around T_c , as clearly seen in Fig. 2(b).

To demonstrate the correlation between the spin configuration and the resistivity, we show in Fig. 3 the temperature- and field-induced magnetizations for the $x=0.175$ crystal and their changes in resistivity. There is seen a minimal remnant behavior in the M-B curve for the spin ordered phase in the metallic $\text{La}_{1-x}\text{Sr}_x\text{MnO}_3$ crystals. Therefore, we show in Fig. 3(a) temperature dependence of the saturated magnetization and the resistivity which were both measured at the bias field of $B=0.5$ T. In Fig. 3(b), on the other hand, the magneti-

zation immediately above T_c is plotted against the magnetic field (B) together with the corresponding resistivity change. From these experimental results, we can deduce the change of the resistivity as a function of the magnetization which represents the averaged ordered moment of the sum of the t_{2g} local spin and forcedly aligned e_g spin on the same Mn site. The result for the $x=0.175$ ($n=0.825$) crystal is shown in Fig. 4, in which the magnetization on the abscissa is normalized by the classical value ($4\mu_B$) in the case of the $n=1$ filling of the e_g band.

Looking at the ρ - M curve, one immediately notices that the experimental points taken at different temperatures (above T_c) draw approximately identical curves in spite of seemingly very different MR behaviors (see Fig. 2(b)). Furthermore, the ρ - M curve, which was obtained using the $\rho(T)$ and $M(T)$ data shown in Fig. 3(a), shows a similar trace. (The $\rho(T)$ curve measured at 0.5 T was scaled in Fig. 4 so that the $\rho(T)$ maximum around T_c coincided with the MR data points.) This fact indicates that the temperature dependence of ρ below T_c (apart from the low-temperature ($T \ll T_c$) region) is also governed by a scattering process similar to the case of the MR above T_c .

In previous studies, the MR in manganese oxides was calculated with use of phenomenological (e.g., Drude-like) assumptions of the s - d model⁷ or the Kondo lattice model,⁸ which gave the relation $\rho(M)/\rho(0) = 1 - (M/M_s)^2$ when $M \ll M_s$ ($=2\mu_B$). However, such a relation, which is depicted by the dashed line ("weak coupling") in Fig. 4, obviously fails to explain the observed behavior even in the small M -region. Recently, one of the present authors (N.F.)¹¹ has derived the exact solution for the ferromagnetic Kondo lattice model (eq. (1)) in the infinite dimension ($D=\infty$) and with $S=\infty$, i.e., classical, spins for arbitrary values of the Kondo coupling (J) and the band filling of the conduction electrons. Application of such a model to the present manganese oxides means that we ignore the quantum fluctuation of the finite-value ($S=3/2$) local spins (t_{2g} state) as well as the spatially correlated multiple scattering effect in the real three-dimensional lattice. We show in Fig. 4 the result of the $S=\infty$, $D=\infty$ model calcula-

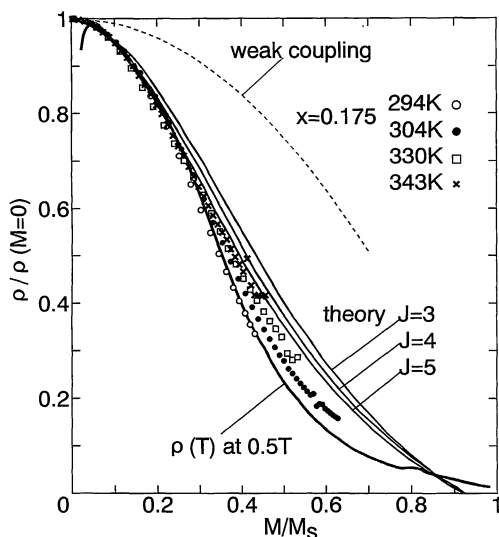


Fig. 4. Normalized resistivity change $\rho(M)/\rho(0)$ as a function of the magnetization (M) per Mn site. The $\rho(T)$ curve measured in the bias field of 0.5 T is also plotted as a function of M with an appropriate scaling to the magnetoresistance data (see text). Theoretical curves with $J=3, 4$, and 5 indicate the results obtained using the $S=\infty$ and $D=\infty$ Kondo lattice model, J being the coupling constant normalized by the one-electron bandwidth (see eq. (1)). The dashed line represents the weak coupling case ($J \rightarrow 0$) and coincides with the curve calculated in previous works (see text).

tion for the normalized resistivity with use of the Kubo formulae as a function of the normalized magnetization (M/M_s). In the calculation, the band filling of the conduction electrons was set at $n=1-x=0.825$ in accord with the experiment, and the density of states of the conduction electron band is assumed to be of a Lorentzian shape. All the possible finite-temperature effects on the conduction electrons are ignored since they are expected to be negligibly small compared with the magnetization-dependent effect within the present $D=\infty$ and $S=\infty$ model.

In spite of the simplified modeling, the experimentally observed universal ρ - M curve is well reproduced by the calculated result. We note that the variation in the J -value (in units of the one-electron bandwidth) does not alter the result significantly, as exemplified by the case of $J=3$ –5, as long as the system remains in the strong coupling regime ($J \gg 1$). Incidentally, the weak coupling limit ($J \rightarrow 0$; shown by the dashed line in Fig. 4) in the present theory reproduces the aforementioned relation $\Delta\rho/\rho(0)=1-(M/M_s)^2$, which is obviously not the experimentally observed case. The essence of the MR effect in the present system can thus be explained quantitatively in terms of the spin-configuration dependent scattering of the conduction holes within the framework of the Kondo lattice model. Nevertheless, a clear and systematic difference between the observed results and calculated curve is observed in the high- M region: The observed MR is generally larger than the calculated one. Part of such a discrepancy may arise from neglect of the quantum fluctuation of t_{2g} spins and the spatially correlated carrier scattering which are suppressed by the magnetic field.

As a final remark, we mention the filling dependence of the MR effect. A similar or even larger MR effect is also observed for the $x=0.15$ crystal near the compositional boundary of the nonmetal-metal transition. For example, the negative MR value ($-\Delta\rho/\rho(0)$) exceeds 0.95 around T_c ($=247$ K) at 15 T for this crystal. When the hole concentration (x) is increased above $x=0.2$, however, the negative MR becomes smaller. We estimated the MR magnitude in the small magnetization region ($M/M_s \leq 0.2$) by using the scaling function $\rho/\rho(0)=1-C(M/M_s)$. Then, the coefficient

C is about 4 for $0.15 \leq x \leq 0.2$, but is observed to decrease to about 2 for $x=0.3$ and about 1 for $x=0.4$. In other words, the deviation of the band filling from $n=1$ seems to drive the system towards the weak coupling ($C=1$) regime. Such a critical filling dependence is also characteristic of the Kondo lattice system with ferromagnetic coupling.¹¹⁾

We are grateful to K. Tomimoto and J. Akimitsu for their help in the microprobe analysis and to H. Yoshizawa for the neutron diffraction characterization of the single crystals. This work was partly supported by a Grant-in-Aid for Scientific Research from the Ministry of Education, Science and Culture, by the Joint Research Program at the Institute for Materials Science, Tohoku University, and by the New Energy and Industrial Technology Development Organization (NEDO).

References

- 1) G. H. Jonker and J. H. Van Santen: *Physica* **16** (1950) 337.
- 2) E. O. Wollan and W. C. Koehler: *Phys. Rev.* **100** (1955) 545.
- 3) C. Zener: *Phys. Rev.* **82** (1951) 403.
- 4) P. W. Anderson and H. Hasegawa: *Phys. Rev.* **100** (1955) 675.
- 5) P.-G. de Gennes: *Phys. Rev.* **118** (1960) 141.
- 6) K. Kubo and N. Ohata: *J. Phys. Soc. Jpn.* **33** (1972) 21.
- 7) C. W. Searle and S. T. Wang: *Can. J. Phys.* **47** (1969) 2703.
- 8) K. Chabara, T. Ohno, M. Kasai and Y. Kozono: *Appl. Phys. Lett.* **63** (1993) 1990.
- 9) S. Jin, T. H. Tiefel, M. McCormack, R. A. Fastnacht, R. Ramesh and L. H. Chen: *Science* **264** (1994) 413.
- 10) R. von Helmolt, J. Wecker, B. Holzapfel, L. Schultz and K. Samwer: *Phys. Rev. Lett.* **71** (1993) 2331.
- 11) N. Furukawa: *J. Phys. Soc. Jpn.* **63** (1994) 3214.
- 12) Note that the structural phase transition temperature decreases from 380 K to 190 K with increase of x from 0.150 to 0.175. The temperature range of the transition as judged from the resistivity change is less than 10 K in each sample, implying that the compositional inhomogeneity is perhaps less than 0.002.
- 13) A different carrier localization effect is observed for the $x=0.15$ crystal in the spin-ordered phase below $T_c=150$ K (see Fig. 1), in which the nearly full magnetic moment ($3.8 \mu_B$ per Mn site) is similarly observed under the magnetic field of approximately 0.2 T as in the metallic samples with higher x . This is perhaps Anderson localization of the fully spin-polarized e_g holes due to the poor screening effect of the random Coulomb potential arising from doped Sr.